Probe Report: Small Molecule Activator of Prostate Cell Differentiation

Project Title: Activators of Prostate Cell Differentiation
Grant Number: NIH 1 X01 MH078937-01

Screening Center Name: New Mexico Molecular Libraries Screening Center
Principal Investigator of Screening Center: Larry A. Sklar, Ph.D., University of New Mexico

Assay Submitter & Institution: Todd A. Thompson, Ph.D., University of New Mexico

PubChem AIDs: 795, 1069, 1076, 1196, 1197,1198, 1200, 1260 (Summary)

Assay or Pathway Target: Phenotypic Assay for Prostate Cell Differentiation

Probe PubChem Compound Identifier (CID): 3240581

Mode of Action: Induces secretory vesicle accumulation associated with prostate cell differentiation.

Overview: The lymph node cancer of the prostate (LNCaP) human cell line is a well-defined prostate cell model. Moreover, it is one of only a few human prostate cell lines that are androgen-responsive. The biphasic androgenic response is characterized by increased growth rate in response to low concentration exposure, and a growth-arrested phenotype at higher physiologic concentrations. We have established a well-defined assay wherein LNCaP cells display the growth-arrested phenotype after incubation with $\geq$ 1nM R1881 (methyltrienolone), a synthetic androgen. Growth-arrested LNCaP cells are viable, accumulate in G1, and exhibit increased intracellular granularity that likely correlates with increased secretory vesicles. This system offers a means for identifying small molecules that affect this phenotypic change since the increased intracellular granularity that accompanies growth-arrest can be accurately measured using flow cytometry. Currently, the discovery of novel chemicals with possible therapeutic utility relies on assays amenable to high throughput screening (HTS). Using the HyperCyt® high throughput flow cytometry screening platform we identified a piperidine carboxamide substituted aryl-oxazole (**CID 3240581; SID 4246202**) that consistently induced increased intracellular granularity in LNCaP cells after four days in culture. Counter-screen analysis with the non-androgen responsive PC-3 prostate cancer cell line suggested that **3240581** affects granularity through an androgen-independent mechanism. Dose response analysis of **3240581** confirmed our initial results and indicated an EC_{50} range of 1–6 microM where LNCaP cells were consistently more affected than PC-3 cells. Microscopic analysis confirmed that **3240581** induced vesicle accumulation in both PC-3 and LNCaP cells. While maximal responses could be achieved at concentrations above 10µM, significant toxic affects were also observed at these concentrations.

Assay Provider Information

Specific Aims:

The assay described in this probe report is based on the observation that androgen-induced differentiation of LNCaP human prostate cancer cells correlates with intracellular granularity, an end-point that can be accurately measured using flow cytometry. Increased ratios of proliferative to differentiative epithelial phenotypes accompany both benign prostatic hyperplasia and prostatic adenocarcinoma. Therefore, defining the cellular mechanisms that result in prostatic epithelial differentiation is crucial to our understanding of these pathophysiological states. Specific Aim #1 of

this project was to screen for small molecules that modulate prostate cell differentiation, using HyperCyt® high throughput (HT) flow cytometry. Intracellular granularity in the LNCaP cell differentiation model served as the phenotypic endpoint for induction of prostate cell differentiation. Specific Aim #2 was to counter-screen active compounds identified in the primary and confirmatory screens in LNCaP cells in a similar dose response assay using PC-3 cells to identify small molecules that induce intracellular granularity in an androgen-independent manner. The discovery of compounds that do not require androgen receptor activation to induce increases in intracellular granularity in prostate cancer cells would suggest that androgen-specific pathways are not necessary for this differentiative change to occur.

Significance:

Prostate cancer contributes significantly to cancer-related deaths in the United States (1). Although there is no known etiology (2), prostatic adenocarcinomas are thought to develop from accumulations of intraepithelial neoplastic lesions known as PINs (3). Adenocarcinoma of the prostate is the most common malignancy of the male urinary tract and its incidence has more than doubled in the last decade (4). While many of these tumors occur in elderly men and have a long doubling time, prostatic carcinoma in younger individuals is often more aggressive and life-threatening (5). Moreover, despite increased clinical study, the molecular basis of this disease is poorly understood (6). One of the main focuses of oncologic study is cellular proliferation and numerous biochemical pathways involving a plethora of intracellular proteins that play important roles in controlling cell growth and viability have been identified. Another facet of cell physiology that impacts oncogenesis is terminal differentiation, and the incomplete progression of prostate epithelial cells to terminal differentiation is considered central to prostate oncogenesis.

Prostate epithelium consists of at least two cell-types; a proliferative basal cell and a luminal secretory cell. The standard model of prostate epithelial differentiation proposes a linear scheme in which cells residing in the basal layer give rise to irreversibly growth-arrested, terminally differentiated, luminal secretory cells by passage through a transit-amplifying intermediate stage of development (6,7). Most prostate cancer cells express luminal cell-specific markers such as cytokeratins 8 and 18, as well as prostate-specific antigen (8); however, cells co-expressing both basal and luminal markers have also been identified (9). While these data suggest that prostatic adenocarcinomas originate from transit-amplifying intermediate epithelial cells, other models have been proposed including hypotheses that posit a primary role for prostate stem cells (6). Identifying agents that disrupt or modulate one or more of the critical biochemical pathways involved in prostatic epithelial differentiation should increase our understanding of prostatic oncogenesis and aid in the development of clinical targets, especially if these novel compounds bypass androgen receptor activation.

Rationale:

Secretory cells such as luminal prostate epithelia, produce, store and release vesicles. Recent studies have determined that the production of prostate cell storage vesicles, containing serous secretions and prostasomes, can be modulated by boric acid, synthetic androgen, and anchorage-dependent growth (10-12) . Increased vesicle formation results in increased light scattering properties of cells that can be detected by flow cytometry. LNCaP cells are well defined, and constitute one of only a few human prostate cell lines that are androgen-responsive (13). The biphasic androgenic response is characterized by increased growth rate in response to low concentration exposure, and a growth-arrested phenotype at higher physiologic concentrations (14). LNCaP cells also respond to increasing concentrations of androgen by increasing their vesicle

content (11). Based on this finding, we designed an HTS assay using HyperCyt®, a high throughput flow cytometry platform (15), where LNCaP cells, cultured in the presence of individual small molecules, are assessed for increases in side scatter. We expect this assay will identify molecules that cause increased production and/or accumulation of prostate secretory vesicles. Hopefully, identified molecules will open up new avenues of investigation related to secretory cell differentiation and vesicle production and release.

Background:

In 2005, over 230,000 men are estimated to develop prostate cancer in the United States. Of these, over 10% will die from their cancer, making prostate cancer the most common malignancy and second leading cause of cancer deaths among men (1, 2). The glandular function of the prostate is to produce secretions that contribute to seminal fluid and may assist in male fertility. Materials secreted by the prostate gland include substances such as prostatic secretory proteins, polyamines, citrate, and zinc. Morphologically, the glandular component of the prostate gland consists of two layers; a basal cell layer that abuts the basement membrane and a secretory cell layer of columnar epithelial cells that produce prostatic fluid. Prostate progenitor cells are believed to reside in the basal cell layer.

Interestingly, 85% of cancers arise from glandular tissues. Biologically, the term differentiation has multiple meanings (reviewed in 16). Differentiation applied to glandular tissues in the mature organism refers to the natural development of functional organ activity among cells within the organ. Terminal differentiation uniquely refers to the process where a cell has achieved a fully differentiated state that is irreversibly growth-arrested. Ultimately, terminally differentiated cells within a tissue die. Cancer cells arising from glandular tissues have subverted the process of terminal differentiation. Therefore, if terminal differentiation can be initiated in cancer cells, it would serve as a useful modality for cancer treatment. However, the molecular pathways driving terminal differentiation are poorly understood.

The primary therapy for advanced prostate cancer is androgen ablation, which prolongs lifespan by delaying prostate cancer progression. Unfortunately, advanced prostate cancers eventually become refractory to androgen ablation therapy. The discovery of molecular probes that demonstrate androgen-independent induction of prostate epithelial differentiation would be useful in identifying new pathway targets for advanced prostate cancer.

Among the known small molecules that are believed to affect prostate cell differentiation, their utility for treating prostatic diseases is disappointing. These include androgens, vitamin A, and vitamin D, all known to activate nuclear receptors (11,14,17,18). A limited number of other small molecules that induce prostate cell differentiation have not yielded information regarding their pathway target(s), for example, butyrate. Although many of these agents induce prostate cell markers of differentiation, it is unclear that these agents have induced terminal differentiation, a critical characteristic for therapeutic candidates. The use of androgens as treatment for prostate cancer has been associated with the promotion of cancer in some prostate cells. Vitamin D has been pursued as a means of promoting prostate cell differentiation, however it is associated with hypercalcemic toxicity. We have shown that less calcemic analogs of vitamin D may be useful in prostate cell differentiation therapy using the LNCaP model (18), yet these analogs still possess substantial toxicity. Therefore, the identification of agents that induce prostate differentiation without toxicity or cancer promotion would be highly beneficial. Expanding the regimen of small molecules that modulate prostate cell differentiation would greatly facilitate these efforts.

Screening Center Information

Assay Implementation and Screening

PubChem BioAssay Name**:** MLSCN Assay for Activators of Prostate Cell Differentiation

List of PubChem Bioassay Identifiers (AIDs): 795, 1069, 1076, 1196, 1197, 1198, 1200

PubChem Primary Assay Description (AID 795)

The assay is conducted in 384-well tissue culture plates in a total volume of 100µl. LNCaP cells (ATCC # CRL-1740) are re-suspended at a concentration of $1x10^5$/mL in assay medium (low glucose DMEM supplemented with 1% FBS, 4% charcoal-stripped FBS, Pen/Strep/Fungizone, L-glutamine) and 99µl are placed in individual wells 18 hours prior to the addition of test compounds. Plates are configured as follows: column one, negative control, cells incubated with 1%DMSO; column two, medium only; columns 3-22, 10µM test compounds; column 23, positive control, cells incubated with 10nM R1881; column 24, medium only. Plates are incubated for 4 days in a humidified 5% CO_2 atmosphere after which assay medium is removed and LNCaP cells are harvested by trypsinization (30µL 0.25%/15 min). Individual wells are sampled using HyperCyt® high throughput flow cytometry. Both forward and side light scattering properties of treated LNCaP cells are measured using a 488nm laser. HyperCyt® sampling of a single 384-well plate is completed in less than 15 min. Acquired data are analyzed using IDLQuery software, developed by Bruce Edwards and available at the NM MLSCN. IDLQuery scans the acquired data and delineates 384 time-resolved, individual samples. Demarcation of change in granularity is made by pooling all samples from column 1. These negative control samples are defined as a population where 10% of the cells exhibit increased granularity based on side scatter properties (i.e., negative control samples exhibit 10% side scatter shift). A gate is set reflecting this distinction that is then applied to each data cluster. These values are exported to a Microsoft Excel spreadsheet template that calculates percent side scatter shift in individual treated samples.

Compounds from missing wells (less than 30 events counted for these wells) were given PUBCHEM_ACTIVITY_OUTCOME = 4.

Compounds were considered "Actives" if the % side scatter shift was greater than 30%. PUBCHEM_ACTIVITY_OUTCOME is indicated as 2 for "Actives" and 1 for "Non-Actives".

The PUBCHEM_ACTIVITY_SCORE was based on the percent side scatter shift. Hence: PUBCHEM_ACTIVITY_SCORE = %side scatter shift

Comments: When less than 30 events (i.e., cells) were collected from a well, the compound test was demeaned missing, and the word "Missing" is entered in the column labeled PUBCHEM_ASSAYDATA_COMMENT to flag these compounds.

Center Summary of the Primary Screen

The primary screen was based on the biphasic response of LNCaP cells to the synthetic androgen R1881, which elicits a proliferative phenotype at low concentrations, while higher concentrations result in growth arrest and a concomitant increase in intracellular granularity. Results

of the primary high throughput screen (HTS) of 24,718 compounds identified 134 compounds (0.5%) that satisfied the hit selection criteria (>30% shift in cellular side scatter shift) regarding increased LNCaP granularity (AID 795). An additional 191 compounds were designated as 'missing' based on an individual well event count that was less than 30. These findings led to the identification of 430 compounds of interest: 134 'actives', 191 'missing' compounds and 105 additional family members based on commonality observed during sub-structure analysis.

Probe Optimization

Three additional single-point screens were performed on LNCaP cells as described above on these 430 compounds, one at 100µM and two at 10µM. Using the selection criteria discussed above, these additional screens resulted in the selection of 72 compounds that increased LNCaP granularity (AID 1069). An additional 23 compounds that consistently resulted in a low event count were also selected for further analysis following these three single point screens (AID 1076).

Description of secondary screens used to optimize probe structure

These 95 compounds were tested in a dose response format using both LNCaP and PC-3 cells (AID 1196, 1197, 1198, 1200). Each compound was serially diluted 1:3 in DMSO six times resulting in seven different final concentrations; the highest of which was 30µM. Each compound concentration was replicated four times resulting in 28 separate data points. In some cases individual data points were either determined to be statistical outliers or were the product of less than 30 event counts and were excluded from analysis. The resulting trends were fitted by Prism(R) software (GraphPad Software, Inc., San Diego, CA) using nonlinear least-squares regression on a sigmoidal dose response model with variable slopes (four parameter logistics equation). Curve fit statistics reported concentration of compound at 50% effect (EC_{50}), low and high boundaries of the 95% confidence interval of the EC_{50}, the Hill Slope, and the correlation coefficient (RSQR). Reporting of EC_{50} estimates were made only for compound data that converged in Prism fitting with a 95% confidence interval, and whose maximum response was greater than 10%. Compounds were considered "Actives" if the estimated EC_{50} for side scatter shift was smaller than 10µM. These data led to the identification of a sub-set family of aryl-oxazoles that consistently increased cellular granularity of which **3240581** was chosen for further analysis.

Probe optimization included a round of secondary dose response screening using the PC-3 androgen non-responsive prostate cancer cell line. Data shown in figures 5 and 6 below characterize the phenotypic responses induced by **3240581** in both LNCaP and PC-3 prostate cancer cell lines.

Chemical characterization of 3240581

The probe candidate was synthesized in bulk by ChemDiv and the biological activity was subsequently confirmed, as described below. The synthetic scheme of the product is shown in figure 3 and structural characterization is shown in figure 4a-d. Starting from the Boc-protected 4-piperidinecarboxylic acid, a carbodiimide coupling with N,N-diisopropylaminoethylamine afforded the amide intermediate which was then deprotected and coupled with 5-(chloromethyl)-4-methyl-2-(4-chlorophenyl)-1,3-oxazole to yield **3240581**.

Figure 1.

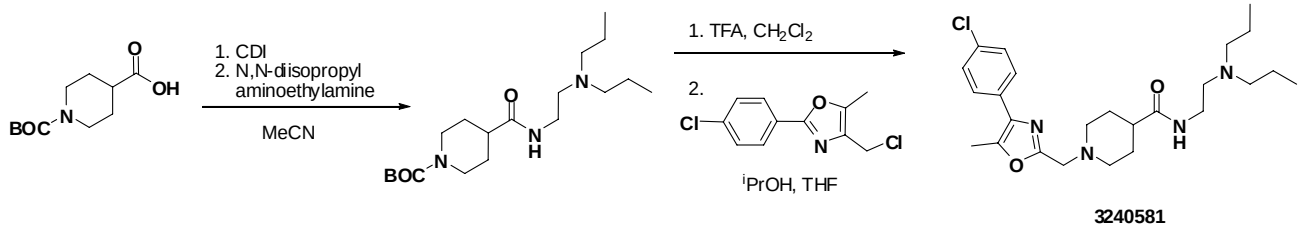

Figure 2a-d.

(a) FT-IR

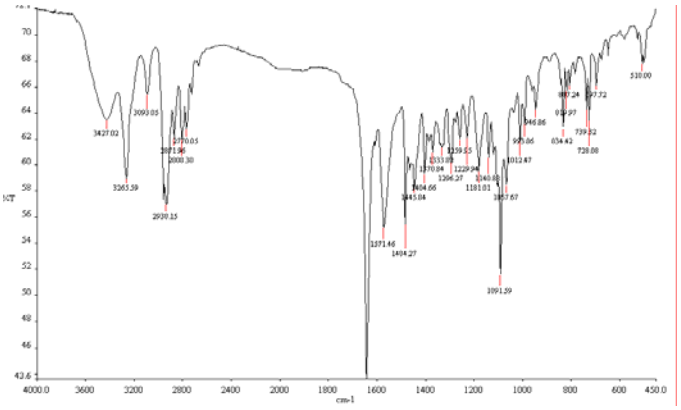

(b) ^1H NMR

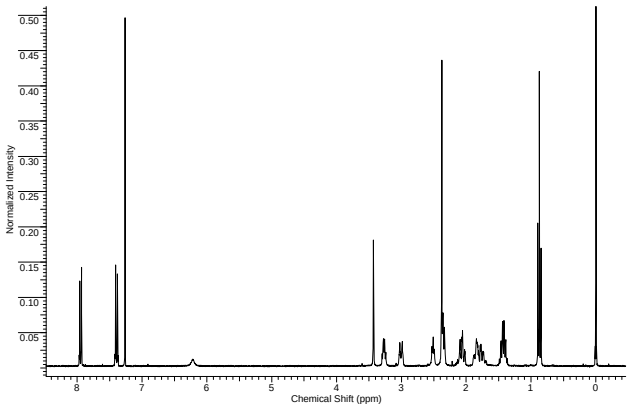

(C522-0766/cid 3240581/sid 4246204): White solid, mp 104-106˚C; **(a)** FT-IR (KBr, cm-1) 3265(w), 2938(m), 1643(s), 1571(m), 1091(s). **(b)** ^1H NMR (300 MHz, $CDCl_3$) δ 7.95 (d, *J* = 8.8 Hz, 2H), 7.39 (d, *J* = 8.8 Hz, 2H), 6.21 (bs, 1H), 3.43 (s, 2H), 3.29-3.24 (m, 2H), 3.03-2.97 (m, 2H), 2.50 (t, *J* = 5.4, Hz 2H), 2.38-2.33 (m, 6H), 2.10-2.01 (m, 3H), 1.88-1.69 (m, 5H), 1.48-1.36 (m, 4H), 0.87 (t, *J* = 7.3 Hz, 6H).

(c) HPLC PDA (top) and ESI-MS (ES+) TIC (bottom)

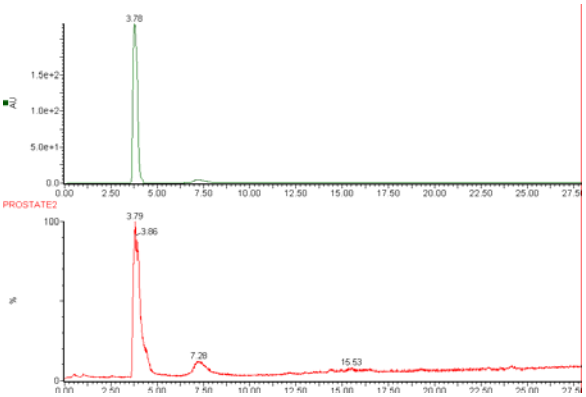

(d) ESI-MS (left) and UV-Vis (right)

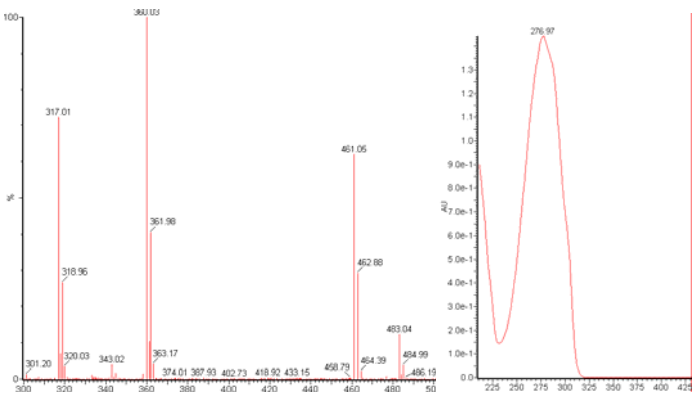

(C522-0766/cid 3240581/sid 4246204): White solid, mp 104-106˚C; **(c)** LC-MS: Eluted from a Waters Symmetry® C_{18} 5µm 3.0 X 150mm column with 13-83% CH_3CN in H_2O (2.33% min-1) containing 0.01% formic acid, RT = 3.78 min. **(d)** UV-Vis at RT =3.78 min. λmax 276 nm. ESI-MS *m/z* (ES+) calcd for $C_{25}H_{37}ClN_4O_2$ $(M+H)^+$ 461.26, found 461.05.

Center summary of probe properties and recommendations for the scientific use of probe as research tool

3240581 is a novel small molecule that induces the accumulation of intracellular vesicles in both LNCaP and PC-3 prostate cancer cell lines. This increase results in increased light scattering properties that can be evaluated using flow cytometry. Figure 5 shows representative dose response analyses for both cell lines. **3240581** was tested in dose response experiments essentially as describe above in the protocol section. Briefly, cells were incubated for four days in the presence of test compound or 1%DMSO. Treated samples were harvested by trypsinization and each sample was analyzed by flow cytometry. Each data point represents a unique sample where approximately 3000 cells were evaluated. Negative control samples treated with 1%DMSO were defined as a population where 10% of the cells exhibit increased granularity based on side scatter properties. This gate was then applied to each treated sample. The EC_{50} for LNCaP cells and PC-3 cells was 1.03µM and 2.3µM, respectively.

Figure 3.

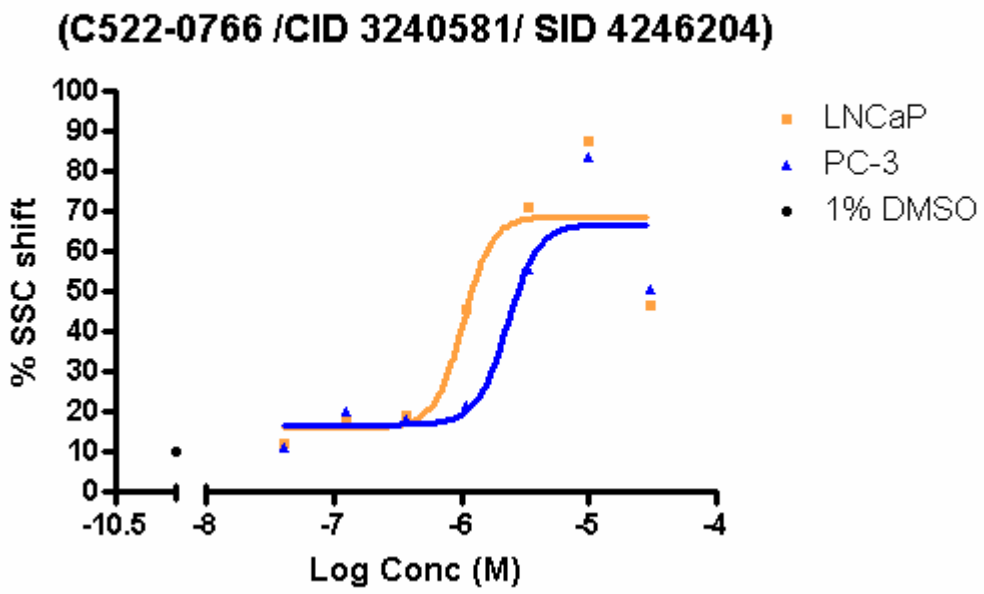

Microscopic evaluation of selected treatment levels of **3240581** is shown in figures 4A - G. For these experiments, cells were seeded onto sterile glass coverslips that were placed into individual wells of a 6 well tissue culture plate. Eighteen hours after this initial seeding differing concentrations of **3240581** were added and the plate was incubated for an additional 4 days. Coverslips were collected and were viewed using a 60X oil immersion objective attached to a BioRad confocal microscope equipped with Lasersharp 2000 software.

Figure 4.

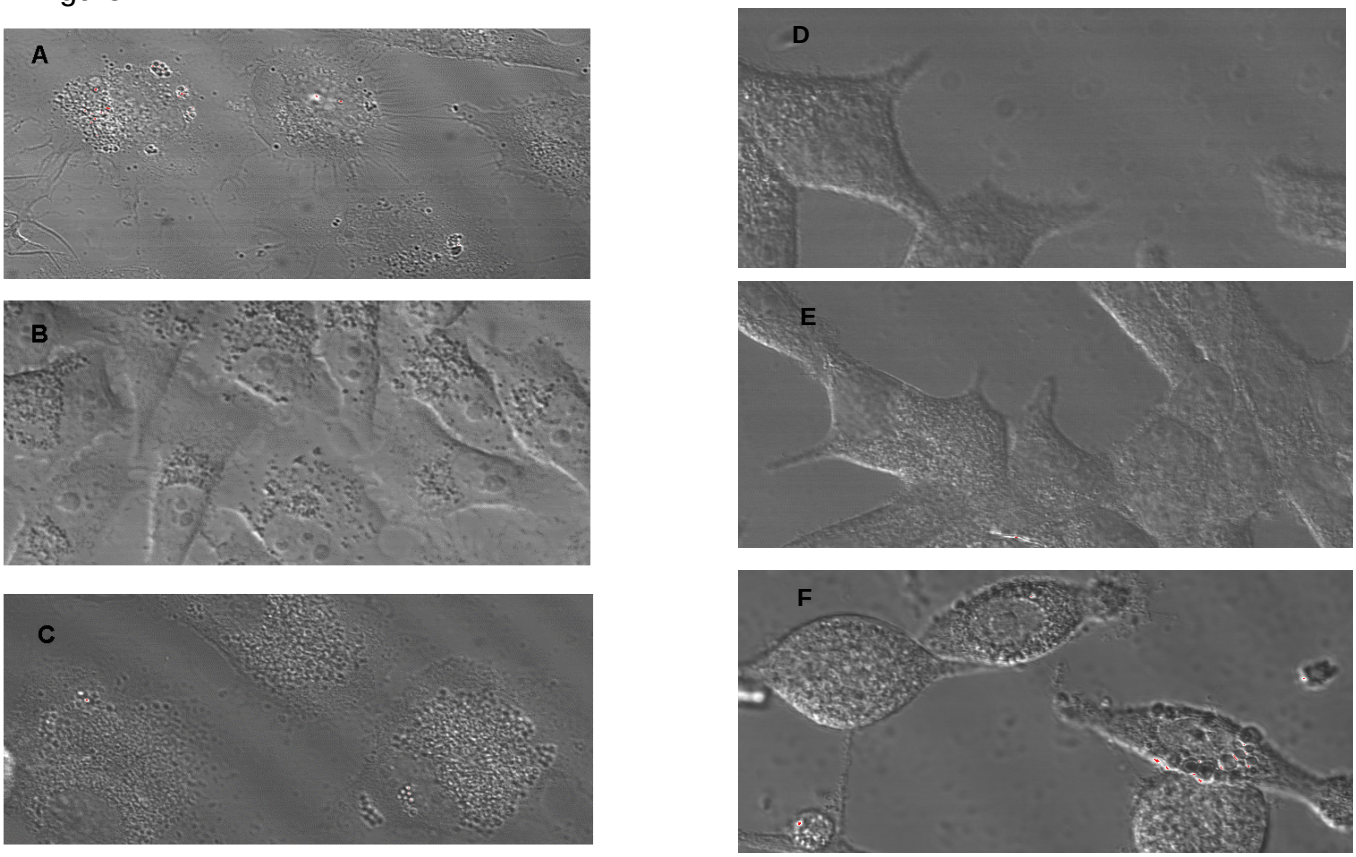

PC-3 cells are shown in figure 6A-C and LNCaP cells in 6D-F. Micrographs A and D show cells treated with 1%DMSO, B and E show cells treated with 1µM **3240581**, and C and F show cells treated with 10µM **3240581**. Note that treatment of cells with **3240581** causes the accumulation of secretory vesicles in both PC-3 and LNCaP cells.

Appendices

Comparative data on probe, similar compound structures and prior probes

A common set of structural features was shared by compounds reported as active from the primary screen. This grouping afforded a general scaffold with a heterocyclic moiety (typically aromatic) and a tertiary amine (predominantly alkyl substituted) separated by an aliphatic amide linker. Narrowing the set of actives down by sub-structure resulted in a family wholly represented by these features (Family 1), as well as representative members of other structural families (Families 2 and 5) and a few singletons. Figure 1 illustrates the basic scaffolds for comparison with the family sub-structure shown in blue. Families 1 and 2 were clustered around their respective aryl-substituted heterocycles and Family 5 was clustered around the N-aryl piperidine subgroup.

Figure 5.

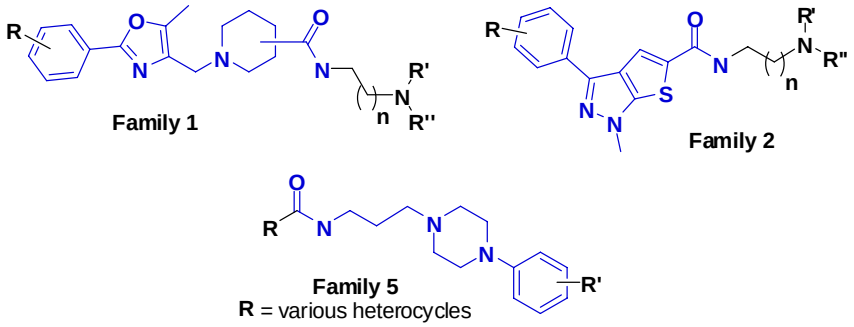

The steric and electronic profiles of these compounds were comparatively similar, however their relative significance was first assessed based on the overall family activity. Family 1 will be discussed in further detail below. Of the 30 members of Family 2 tested, less than a third were selected for follow-up, of which two compounds (Figure 2) were confirmed by dose response with the best (**CID 5308230, SID 7966622**) having an EC_{50} of 5.53 µM. Despite the commonality across the two hits, the lack of activity in the confirmatory screen within the family ruled out further exploration. Family 5 was the most structurally varied of the families due to its simple scaffold. Several of its 74 members were selected for follow-up in dose response. Two compounds similar to the Family 1 and 2 hits were found to be active and the best (**CID 5308205, SID 7966399**) demonstrated a less than micromolar efficacy. However, due to the general lack of activity in the set, coupled with the apparent promiscuity in PubChem of its members, this family was also not explored further. None of the similarly structured singletons were confirmed in the dose response.

Figure 6.

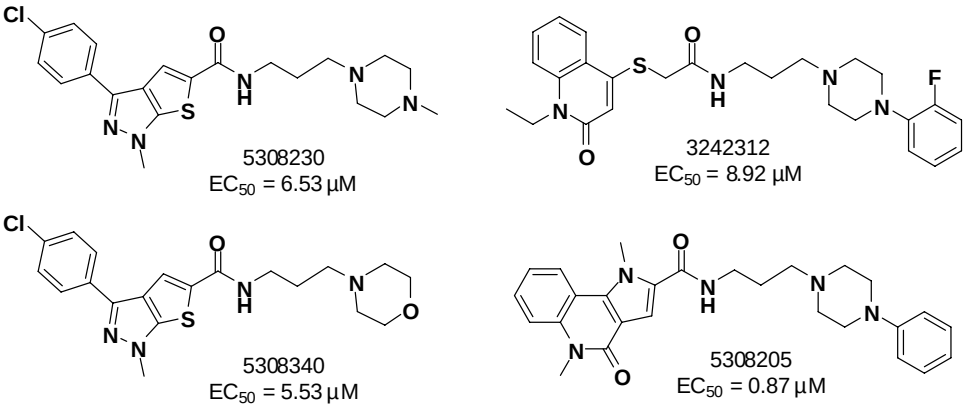

Family 1 contained the most active compounds of all the subsets. Table 1 illustrates the Family 1 members screened and their corresponding biological data which includes single point information as well as dose response data. The scaffold is broken into three regions: Region 1 (R^1) represents the substituent on the aryl oxazole, Region 2 (R^2) is the N-substituent on the carboxamide, and the third region is simply the regioisomer of the piperidine substitution.

Due to distribution limitations of R^1 relative to R^2 it is difficult to make solid conclusions about the effect of R^1 substitutions. Although somewhat arbitrary, we can still look at the proportion of a given R^1 group in the total family set versus the active compound subset. For instance, the 2-fluoro and 3-chloro groups represent 7 and 16 compounds, respectively, but show no activity in confirmatory

dose response. Thus it is likely that these are less active R^1 functions. Unlike 2-fluoro and 3-chloro which are relatively well distributed versus R^2, 3-methyl (4 total members) is only represented in the inactive R^2 alkyl analogs. Thus, 3-methyl cannot be considered a problematic substitution for R^1 based on this limited information. The two R^1 substituents with the most dose response confirmed active compounds are 4-chloro and 2-methyl. Both of these substituents demonstrate approximately double the representation in the actives category as they do members of the total tested group (1:2, family member to actives). This speaks well for their worth as functional groups capable of increasing substrate activity.

A similar rational can be used to discuss the piperidine substitution. About a third of the family members are 1,3-substituted and only 1 of these is a confirmed active (Entry 11). The analogous 1,4-compound (Entry 10) is in the same range of activity (7.03 vs. 6.69 µM respectively) as it's 1,3 counterpart, but the 4-chloro-1,4-analog (Entry 9) is significantly more potent. The 1,4-substitution appears to be the preferential regioisomer. It's important to note however that the overall three dimensional morphology is likely much more complex than this simple analysis for both the R^1 substituent as well as the piperidine substitution.

A variety of R^2 substituents were screened with the best activity being seen with alkyl-linked tertiary amines (Entries 1-3, 5, 6, 9-11, 18, 19). Entries 1 and 2, both simple alkyl amines, were the most active compounds and Entry 1 demonstrated a sub-micromolar EC_{50} of 770 nM. Entries 3, 5, and 6 were also relatively simple alkyl amines but resulted in lower activities and had poor statistical curve fitting due to apparent cell toxicity. The morpholine function of Entries 9-11 also resulted in reasonable activity, albeit worse than their simple tertiary amine counterparts, including the piperizine analog of Entry 6. All other R^2 substituents were less active. One of two benzylic amines, Entry 18, had an EC_{50} of 5.16 µM while aryl amines (Entries 19-23) were generally inactive. The only exception was Entry 19 with an EC_{50} of 2.00 µM but this compound also demonstrated potential toxicity issues. Amides, carbamates, and a furan substituted ketone showed no activity (Entries 4, 12-17). Alkyl-linked heterocyclic substituents also demonstrated low or no activity (Entries 23-30). Alkyl and aryl substituents were completely inactive (Entries 31-41) as were most alkyl-linked aryl substituents (Entries 43-46). Entry 42 with its polarizing *p*-fluoro benzylic substituent was the exception with an EC_{50} of 3.28 µM, however, this compound also demonstrated significant toxicity.

Table 1.

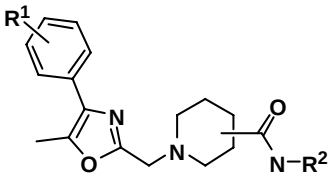

1,3 or **1,4**

Entry	CID #	SID#	R^1	Piperidine Substitution	R^2	Subgroup Members[a]	Activity Score[b]	EC_{50} (µM)[c] (PC3)
1	3240581	4246202	4-chloro	1,4	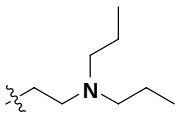	1	99	0.77 (6.50)

Entry	CID #	SID#	R^1	Piperidine Substitution	R^2	Subgroup Members[a]	Activity Score[b]	EC_{50} (μM)[c] (PC3)
2	3239818	4245336	3-bromo	1,4	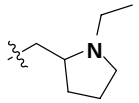	1	47	1.12 (1.16)
3	3245404	4251758	2-methyl	1,4	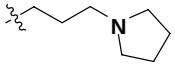	1	38	3.55[d] (1.90[d])
4	5308178	7966356	4-chloro	1,3	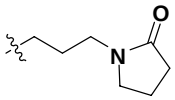	3	28	-
5	3244725	4250981	2-methyl	1,4	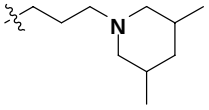	1	99	1.10[d] (1.27)
6	5307204	7964743	4-chloro	1,4	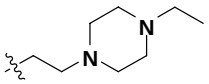	1	50	5.59[d] (6.46)
7	5307943	7965977	3-chloro	1,3	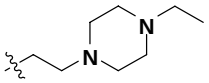	1	41	-
8	5309851	7969240	3-chloro	1,4	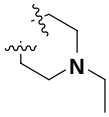	2	33	-
9	3235876	4240817	4-chloro	1,4	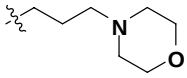	1	41	2.99 (3.44)
10	3237063	4242178	2-methyl	1,4	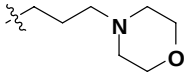	1	47	6.69 (5.47)
11	2999500	4245463	2-methyl	1,3	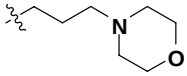	3	49	7.03 (11.67[d])
12	5309532	7968665	4-ethyl	1,4	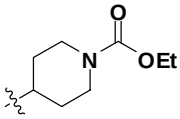	1	-	-
13	5308146	7966305	3-chloro	1,3	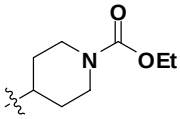	1	26	-
14	5307746	7965655	2-methyl	1,4	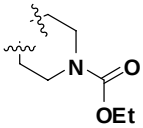	1	40	-
15	5308554	7966992	4-chloro	1,3	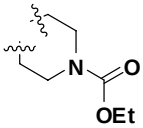	1	17	-
16	5309096	7967890	4-chloro	1,3	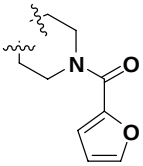	1	37	-

Entry	CID #	SID#	R^1	Piperidine Substitution	R^2	Subgroup Members[a]	Activity Score[b]	EC_{50} (μM)[c] (PC3)
17	5308114	7966254	2-methyl	1,4	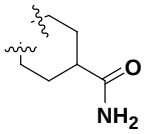	1	21	-
18	5307966	7966024	4-chloro	1,4	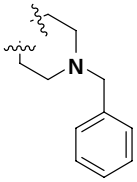	2	48	5.16[d] (1.81)
19	3239890	4245416	4-chloro	1,4	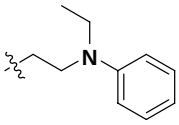	3	45	2.00 (inactive[d])
20	3236673	4250326	4-methoxy	1,3	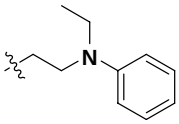	1	42	-
21	3242611	4248543	4-ethyl	1,4	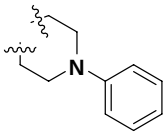	1	37	-
22	5309641	7968862	3-chloro	1,4	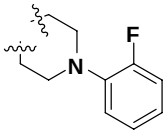	1	-	-
23	3242911	4244735	4-ethyl	1,4	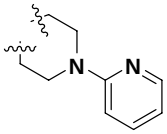	4	42	-
24	3244199	4250380	2-methyl	1,4	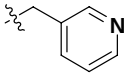	4	44	> 30.0[d] (12.52[d])
25	3237192	4242322	4-chloro	1,3	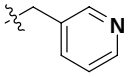	2	29	-
26	3245365	4251712	4-chloro	1,3	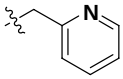	1	31	-
27	3237752	4242962	2-methyl	1,4	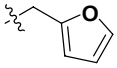	5	44	-
28	3242622	4248554	3-chloro	1,3	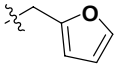	2	36	-
29	3238084	4243349	3-chloro	1,4	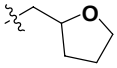	2	42	-
30	3239927	4245458	2-fluoro	1,4	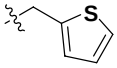	1	43	-
31	3243310	4249346	3,4-dimethoxy	1,4		1	-	-
32	3241024	4246719	2-fluoro	1,4		1	28	-
33	3243295	4249327	3-methyl	1,3		1	26	-

Entry	CID #	SID#	R^1	Piperidine Substitution	R^2	Subgroup Members[a]	Activity Score[b]	EC_{50} (µM)[c] (PC3)
34	3244103	4250265	3-methyl	1,3		1	25	-
35	3244705	4250959	3-methyl	1,3	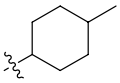	1	23	-
36	3238767	4244125	3-methyl	1,3	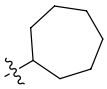	1	37	-
37	3245975	4252422	2-fluoro	1,4	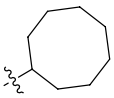	1	16	-
38	3236673	4241736	2-fluoro	1,4	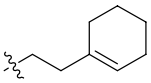	2	40	-
39	3244713	4250968	3,4-dimethoxy	1,4	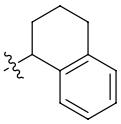	1	-	-
40	5308919	7967603	3,4-dimethoxy	1,4	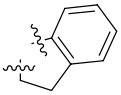	1	12	-
41	5308011	7966088	4-chloro	1,4	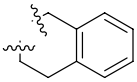	1	39	-
42	3535853	4240790	4-ethyl	1,4	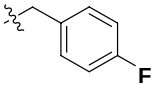	1	28	3.28[d] (inactive[d])
43	3236520	4241563	4-ethyl	1,4	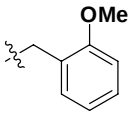	3	32	-
44	5308493	7966878	3-chloro	1,3	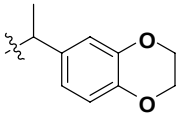	1	9	-
45	3241384	4247146	4-ethyl	1,4	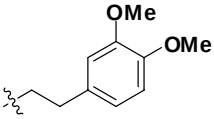	5	43	-
46	3235974	4240937	4-ethyl	1,3	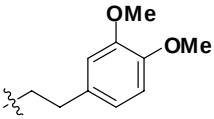	3	33	-

a.) Subgroup is defined as compounds that share the same piperidine regioisomeric substitution and the same R^2 functional group but have R^1 as a variable region. The highest activity member is represented with the other members being less active or inactive. All dose response confirmed actives are listed regardless of sub-grouping.
b.) Activity Score: Compounds were considered "Actives" if the % side scatter shift was greater than 30% and were ranked numerically where higher numbers indicate a greater % shift. A dash in this field indicates a compound that was negative in the primary screen and was not followed up.
c.) EC_{50}: Compounds were considered "Actives" if the estimated EC50 for side scatter shift was smaller than 10 µM. A dash in this field indicates that the compound was not followed up by dose response.

d.) These values have no dose response activity score reported in PubChem due to statistical curve fit issues. Many of these poor curves were the result of low event numbers (i.e. cell death) and thus were adjusted based on low event criteria to allow for an EC_{50} value to be calculated. The values reported here are for SAR comparison purposes.

Table 2. Probe activity reported in confirmation assays

AID	Active	Inactive	Tested	Outcome Method	Name
1200	1		1	Confirmatory	MLSCN Assay for Activators of Prostate Cell Differentiation: Counter Screen Dose Response of Potential Cell Killers
1198	1		1	Confirmatory	MLSCN Assay for Activators of Prostate Cell Differentiation: Primary Dose Response Assay
1196	1		1	Confirmatory	MLSCN Assay for Activators of Prostate Cell Differentiation: Secondary Dose Response Assay
1197		1	1	Confirmatory	MLSCN Assay for Activators of Prostate Cell Differentiation: Primary Screen Dose Response of Potential Cell Killers

Bibliography

1. Jemal A, Murray T, Ward E, Samuels A, Tiwani RC, Ghafoor A, Feuer EJ, Thun MJ. Cancer Statistics 2005. *CA Cancer J Clin* 55:10-30. 2005.

2. United States Cancer Statistics Working Group. 2006. United states cancer statistics: 2003 incidence and mortality. United States Department of Health and Human Services, Centers for Disease Control and Prevention, and National Cancer Institute. Atlanta, Georgia, USA. 451pp.

3. Wiley EL, Davidson P, McIntire DD, Sagalowsky, AI. Risk of concurrent prostate cancer in cryoprostatectomy specimens is related to volume of high grade prostatic intraepithelial neoplasia. *Urology*, 49:692-696. 1997.

4. Lu-Yao GL and Greenberg ER. Changes in prostate cancer incidence and treatment in the USA. *Lancet* 343:251-254. 1994.

5. Burton JL, Oakley N, Anderson JB. Recent advances in the histopathology and molecular biology of prostate cancer. *BJU Int.* 85:87-94. 2000.

6. Lawson DA, and Witte O. Stem cells in prostate cancer initiation and progression. *J. Clin. Invest.* 117:2044-2050. 2007.

7. Tokar EJ, Ancrile BB, Cunha GR, Webber MM. Stem progenitor and intermediate cell types and the origin of human prostate cancer. *Differentiation* 73:463-473. 2005.

8. Okada H, Tsubura A, Okamura A, Senzaki H, Naka Y, Komatz Y, Morii S. Keratin profiles in normal/hyperplastic prostates and prostate carcinoma. *Virchows Arch A Pathol Anat Histopathol.* 421:157-61. 1992.

9. Verhagen AP, Ramaekers FC, Aalders TW, Schaafsma HE, Debruyne FM, Schalken JA. Colocalization of basal and luminal cell-type cytokeratins in human prostate cancer. *Cancer Res.* 52:6182-6187. 1992

10. Barranco WT, and Eckhert CD. Cellular changes in boric acid-treated DU-145 prostate cancer cells. *B. J. Cancer* 94:884-890. 2006

11. Thompson TA, Church DR, Zhong W, Oberly TD, Wilding G. Terminal differentiation induction in LNCaP human prostate cancer cells. *Proc Am Assos Cancer Res.* 45:889. 2004.

12. Carlsson L, Lennertsson L, Ronquist G, Larsson A, Nilson S, Nilsson O. Mode of growth determines differential expression of prostasomes in cultures of prostate cancer cell lines and opens for studies of prostasome gene expression. *Upsala J Med Sci. 111:293-301. 2006.*

13. Horoszwewicz JS, Leong SS, Kawinski E, Karr JP, Rosenthal H, Chu TM, Mirand EA, Murphy GP. LNCaP model of human prostatic carcinoma. *Cancer Res* 43:1809-1818. 1983.

14. Church DR, Lee L, Thompson TA. Basu HS, Ripple MO, Ariazi EA, Wilding G. Induction of AP-1 activity by androgen activation of the androgen receptor in LNCaP human prostate carcinoma cells. *Prostate.* 63:155-168. 2005.

15. Kuckuck FW, Edwards BS, Sklar LA. High throughput flow cytometry. *Cytometry.* 44:83-90. 2001.

16. Studzinski GP and Harrison LE. Differentiation-related changes in the cell cycle traverse. *Int Rev Ctyol* 189:1-88. 1999.

17. Esquenet M, Swinnen JV, Heynes W, Verhoeven G. Control of LNCaP proliferation and differentiation: actions and interactions of androgens, 1alpha25-dihydroxycholecalciferol, all trans retinoic acid, 9-cis retinoic acid and phenylacetate. *Prostate* 28:182-194. 1996.

18. Bauer JA, Thompson TA, Church DR, Ariazi EA, Wilding G. Growth inhibition and differentiation in human prostate cancer cells induced by the vitamin D analog 1-alpha-2,4-dihydroxy vitamin D2. *Prostate* 55:159-167. 2003.